Carbohydrate Polymers 114 (2014) 375–383

Contents lists available at ScienceDirect

Carbohydrate Polymers

journal homepage: www.elsevier.com/locate/carbpol

Optimization of reaction conditions by RSM and structure characterization of sulfated locust bean gum

Junlong Wang[a,b,*], Ting Yang[a,b], Jia Tian[a,b], Wenxi Liu[a,b], Fan Jing[a,b], Jian Yao[a,b], Ji Zhang[a,b,c], Ziqiang Lei[c]

[a] College of Life Science, Northwest Normal University, Lanzhou 730070, People's Republic of China
[b] Bioactive Products Engineering Research Center For Gansu Distinctive Plants, Northwest Normal University, Lanzhou 730070, People's Republic of China
[c] Key Laboratory of Eco-Environment-Related Polymer Materials Ministry of Education, College of Chemistry and Chemical Engineering, Northwest Normal University, Lanzhou 730070, People's Republic of China

ARTICLE INFO

Article history:
Received 21 June 2014
Received in revised form 13 August 2014
Accepted 19 August 2014
Available online 26 August 2014

Keywords:
Galactomannan
Locust bean gum
Sulfation
Solution conformation
Response surface methodology

ABSTRACT

Sulfated derivatives of galactomannan from locust bean gum (LBG) with the degree of substitution (DS) of 0.34–1.07 were synthesized using chlorosulfonic acid/pyridine (CSA/Py) method. Box–Behnken design (BBD) of response surface methodology (RSM) was employed to optimize the reaction conditions. Results of FT-IR and X-ray photoelectron spectroscopy (XPS) indicated that —SO_3H groups were widely present in sulfated LBG (SLBG). ^{13}C NMR result revealed that sulfation had occurred and C-6 substitution was predominant in SLBG. All sulfated samples showed a decrease in M_w and more broad molar mass distribution in size exclusion chromatography combined with laser light scattering (SEC-LLS) analysis. Results of $M_W - \langle S^2 \rangle_z^{1/2}$ showed a decrease in fractal dimension (d_f) value. Laser light scattering results also showed a conformation transition from a compact chain conformation of branched clusters to a random coil conformation of SLBG. Compared to LBG and SLBG with low DS and molecular weight, $SLBG_2$ exhibited an internal structure of random coil with a DS of 1.07. DS and molecular weight had great influence on its conformation in aqueous solution. Our results confirmed that the degradation of polysaccharide and —SO_3H groups improved significantly the stiffness of the chains due to the electrostatic effect.

© 2014 Elsevier Ltd. All rights reserved.

1. Introduction

The biological activity of polysaccharides is being increasingly recognized for human applications (Prajapati, Jani, Moradiya, Randeria, & Nagar, 2013). The study of the relation between chemical structure and biological activities of polysaccharides is one of the most intriguing and challenging scientific endeavors (Tao, Zhang, Yan, & Wu, 2007). It is well known that the activities of polysaccharides are depended upon the chemical structure, such as monosaccharide composition, average molecular weight, degree and pattern of substituting groups and solution conformation (Wu, Li, Cui, Eskin, & Goff, 2012; Tao et al., 2007; Chen, Xu, Zhang, & Kennedy, 2009a). Considerable attention has been paid to the solution conformation of natural polysaccharides (Wu et al., 2012; Yi et al., 2012; Tao et al., 2007; Yang & Zhang, 2009). It is reported that the extended chain conformation were beneficial to enhance the biological activities of water soluble polysaccharides (Chen, Xu, Zhang, & Zeng, 2009b).

Recently, chemical modifications of polysaccharides are generally done for preparing custom-made derivatives having desirable functionality attributes (Parvathy, Susheelamma, Tharanathan, & Gaonkar, 2005). Among the synthetic biopolymers, sulfated polysaccharides represent a class of macromolecules of particular interest. The sulfation of polysaccharides can not only enhance the water solubility but also change the chain conformation, resulting in the alteration of their biological activities (Liu et al., 2009). Many studies have confirmed that sulfated polysaccharides exerted potent biological properties in comparison with non-sulfated polysaccharides, such as anti-coagulant, anti-virus, antioxidant and anti-tumor activities (Wang, Li, & Chen, 2009). It is well known that the structure of modified polysaccharides is depended on the reaction conditions. It suggests that upon interaction with reaction reagent, modified polysaccharide undergoes complex conformational changes that subsequently modify the

* Corresponding author at: Northwest Normal University, College of Life Science, Anning East Road 967, Lanzhou 730070, Gansu, People's Republic of China. Tel.: +86 0 13919168252; fax: +86 0931 7971414..
E-mail address: nuno-vai@163.com (J. Wang).

http://dx.doi.org/10.1016/j.carbpol.2014.08.035
0144-8617/© 2014 Elsevier Ltd. All rights reserved.

biological activities. It is the purpose of the present investigation to explore systematically the solution conformation of sulfated polysaccharides with different structure features.

Galactomannans are polysaccharides consisting mainly of mannose and galactose units. The mannose elements from linear chain linked with galactopyranosyl residues as side chain at varying distances depending on the plant origin (Barak & Mudgil, 2014). The physicochemical properties of galactomannans are strongly influenced by the galactose content and distribution of the galactose units along the main chain. Being a galactomannan, locust bean gum (LBG) has a wide application in pharmaceutical field. LBG mainly consists of a neutral galactomannan polymer made up of 1,4-linked D-mannopyronosyl units and every fourth of fifth chain is substituted on C-6 with a D-galactopyranosyl unit (Prajapati et al., 2013). In our previous studies, sulfated derivatives of galactomannan from guar gum (SGG) were prepared. Antioxidant assays showed that SGG had better antioxidant activities (Wang, Zhao, Wang, Yao, & Zhang, 2012). However, earlier reports were not related to any aspects on synthesis, characterization and solution conformation studies of sulfated LBG.

The present study is focused on the mechanisms governing the relations between structure features and chain conformation. For that purpose, sulfated derivatives of LBG (SLBG) are prepared by chlorosulfonic acid/pyridine (CSA/Py) method. Box–Behnken design (BBD) of response surface methodology (RSM) was employed to optimize the reaction conditions. FT-IR, ^{13}C NMR and X-ray photoelectron spectroscopy (XPS) are employed to characterize the chemical structure of SLBG. Moreover, we also attempt to study the solution conformation of LBG and SLBG using size exclusion chromatography combined with laser light scattering (SEC-LLS). We hope this work can provide valuable information to further understand chain conformation properties of sulfated biopolymers.

2. Materials and methods

2.1. Purification of LBG

The protein of commercial LBG (protein content was 5.6%, weight average molecular weights was 2.313×10^6 g/mol) was removed by Sevage method joined papain according to the reported method (Wang et al., 2010b). The carbohydrate content of purified LBG was 90.07%, determined by phenol sulfuric acid procedure (Wang et al., 2010b). Monosaccharide composition analysis was determined according to the reported method (Wang et al., 2010a). The ratio of mannose to galactose was 3.33:1.

2.2. Sulfated modification of LBG

2.2.1. Preparation of sulfating reagent

Chlorosulfuric acid (CSA) was dropped one by one in anhydrous pyridine filled in three-necked flask, under agitating and cooling in ice water bath (Wang et al., 2010a). Preparation of sulfating reagent was completed in 40 min.

2.2.2. Sulfation reaction

LBG (500 mg) was suspended in anhydrous formamide (5 mL) at room temperature with stirring for 30 min and the sulfating reagents were added dropwise. The mixture was stirred for various durations and/or temperatures as designed by BBD shown in Tables 1 and 2. After reaction, the mixture was cooled to room temperature and the pH was adjusted to 7–8 with 2 mol/L NaOH solution. The mixtures were precipitated with EtOH (95%), washed, redissolved in water and then dialyzed (molecular weight cutoff 8–12 kDa) against tap water for 48 h and distilled water for 24 h to remove pyridine, salt and potential degradation products. Fifteen samples ($SLBG_1$–$SSLBG_{15}$) with different degree of substitution (DS) were collected after lyophilizing.

Table 1
Levels and code of variable chosen for Box–Behnken design.

Variables	Symbol		Levels		
	Coded	Uncoded	−1	0	1
Ratio of CSA to pyridine	x_1	X_1	1/2	1/1	2/1
Reaction time (min)	x_2	X_2	120	180	240
Reaction temperature (°C)	x_3	X_3	40	55	70

The sulfur contents of SLBG were determined by reported method (Wang et al., 2012). A calibration curve was constructed with sodium sulfate as standard. Sulfur content (*S*%) was determined by elemental analysis (Euro Vector EA3000, Leeman). DS was calculated according to the equation.

$$DS = \frac{1.62 \times S\%}{32 - 1.02 \times S\%} \quad (1)$$

2.3. Box–Behnken design of reaction conditions

Box–Behnken statistical design of response surface methodology (RSM) is used to statistically optimize the formulation parameters and evaluate main effects, interaction effects and quadratic effects of the formulation ingredients on the DS of SLBG. According to the principle of Box–Behnken design, ratio of CSA to pyridine (CSA/Py), reaction time and reaction temperature were taken as the variables tested in a 15-run experiment to determine their optimum levels. As shown in Table 1, the three factors chosen for this study was designated as X_1, X_2, X_3 and prescribed into three levels, coded +1, 0 and −1 for high, intermediate and low value, successively. Test variables were coded according to the following equation:

$$x_i = \frac{(X_i - X_0)}{\Delta X} \quad (2)$$

where x_i was the coded value of an independent variable; X_i was the actual value of an independent variable; X_0 was the actual value of an independent variable at centre point; and ΔX was the step change value of an independent variable. DS of SLBG was taken as response. For predicting the optimal point, a second-order polynomial model was fitted to correlate relationship between independent variables and response (DS of SLBG). For the three factors, the equation was

$$Y = A_0 + \sum_{i=1}^{3} A_i X_i + \sum_{i=1}^{3} A_{ii} X_i^2 + \sum_{i=1}^{2} \sum_{j=i+1}^{3} A_{ij} X_i X_j \quad (3)$$

Table 2
Box–Behnken design and the response values for the DS of SLBG.

Run	CSA/pyridine	Reaction time (min)	Reaction temperature (°C)	DS
1	−1	−1	0	0.65
2	1	−1	0	1.07
3	−1	1	0	0.80
4	1	1	0	0.34
5	−1	0	−1	0.68
6	1	0	−1	0.61
7	−1	0	1	0.42
8	1	0	1	0.39
9	0	−1	−1	0.85
10	0	1	−1	0.68
11	0	−1	0	0.68
12	0	1	1	0.61
13	0	0	0	0.92
14	0	0	0	0.85
15	0	0	0	0.97

where Y was the response variables (DS of SLBG), A_0, A_i, A_{ii}, A_{ij} were the regression coefficients of variables for intercept, linear, quadratic and interaction terms, respectively. X_i and X_j were independent variables ($i \neq j$).

Analysis of the experimental design and data was carried out using Design Expert software (Version 8.0.5). Analyses of variance were performed by ANOVA procedure. The fitness of the polynomial model equation was expressed by the coefficient of determination R^2 and its statistical significance was checked by F-test at a probability (P) of 0.001, 0.01 or 0.05. The significances of the regression coefficients were also tested by F-test.

2.4. Characterization of sulfated LBG

2.4.1. FT-IR analysis

The FT-IR spectrum of each sample was measured by using a method as reported by Wang et al. (2014). A known weight of dried sample of each polysaccharide was homogenized with KBr powder and then pressed into pellets for FT-IR spectrum (Thermo Nicolet iS10) measurement in the frequency range of 400–4000 cm^{-1} at a resolution of 4 cm^{-1}. The total number of scans recorded was 16.

2.4.2. NMR spectroscopy

NMR experiments were obtained using a 400 MHz Bruker model Avance spectrometer (DPX-400) incorporating Fourier transform. ^{13}C NMR (100.59 MHz) analyzes were performed at 70 °C with the samples being dissolved in D_2O. The chemical shifts were expressed in ppm relative to the resonance of the internal standard Me_4Si. The sample (10 mg of each) was heated (at 80 °C for 30 min) with water (1 mL), centrifuged and the resulting supernatant lyophilized. The freeze-dried sample was deuterium-exchanged by lyophilisation with D_2O and then examined in 99.9% D_2O.

2.4.3. X-ray photoelectron spectroscopy (XPS)

For chemical composition analysis, samples were characterized using XPS (PHI 5702, USA) with a focused monochromatic Al-$K\alpha$ source (1486.7 eV) for excitation. The pressure in the chamber was below 2.666×10^{-7} Pa (i.e. 2.67×10^{-7} Pa) before the data were taken, the voltage and power of the anode were 15 kV and 200 W, respectively. The take-off angle was set at 45°. The pass energies for survey and multiplex scans were 117.40 and 23.50 eV, respectively. Data analysis was carried out with Multipak software provided by the manufacturer. For quantitative chemical composition analysis, two samples in each group were acquired and the survey scans were performed in two different areas on each sample.

2.4.4. Molecular weight determination

SEC-LLS measurements were carried out on size-exclusion chromatograph combined with multi-angle laser photometer (MALLS, $\lambda = 690$ nm; DAWN EOS, Wyatt Technology Co., USA). Ultrahydrogel™ column (7.8 × 300 mm, Waters, USA) was used. An optilab refractometer (Dawn, Wyatt Technology Co., USA) was simultaneously connected. LBG and SLBG with desired concentrations (0.01 mg/mL) were prepared (dissolved in ultrapure water) and optical clarification of these samples was achieved by filtration into a scattering cell. The injection volume was 50 μL and the flow rate was 0.5 mL/min (mobile phase of ultrapure water). The refractive index increment (dn/dc) value of the sample was determined by using an optilab refractometer at 690 nm (25 °C) to be 0.145 mL/g. The basic light scattering equation was as follows:

$$\frac{KC}{R_\theta} = \frac{1}{M_w}\left(1 + \frac{16\pi^2\langle S^2\rangle_z}{3\lambda^2} \times \sin^2\left(\frac{\theta}{2}\right)\right) + 2A_2C \quad (4)$$

where K was an optical constant equal to $[4\pi^2 n_0^2 (dn/dc)^2]/(\lambda^4 N_A)$; C, the polysaccharide concentration in mg/mL; R_θ, the Rayleigh ratio of the scattered to incident light intensity; M_W, the average molecule weight; λ, the wavelength of incident light; n_0, the refractive index of the solvent; dn/dc, the refractive index increment; N_A, the Avogadro number; A_2, the second virial coefficient; $\langle S^2\rangle_z$, the mean square radius of gyration; θ, the scattering angle. As the column separated the polymer according to molecular size, each fraction was led to the light scattering detector for instantaneous measurement of the scattering intensities. The polymer concentration was calculated based on the peak area determined by the refractive index detector, according to glucan standards.

3. Results and discussion

3.1. Optimization of reaction conditions by BBD

3.1.1. Model and statistical analysis

Response surface optimization is more advantageous than the traditional single parameter optimization because it saves time (Yin & Dang, 2008). There were a total of 15 runs for optimizing the three individual parameters in the current Box–Behnken design which was applied to the sulfation reaction of LBG. The values of response (DS of SLBG) at different experimental combination for coded variables were given in Table 2. The DS ranged from 0.34 to 1.07. By applying multiple regression analysis on the experimental data, the response variable and the test variables were related by the following second-order polynomial equation:

$$Y = 0.91 - 0.018X_1 - 0.10X_2 - 0.090X_3 - 0.22X_1X_2 + 0.010X_1X_3 + 0.025X_2X_3 - 0.19X_1^2 - 0.00091X_2^2 - 0.20X_3^2 \quad (5)$$

where Y was the DS and X_1, X_2 and X_3 were the coded values for three parameters.

The ANOVA of the quadratic regression model showed that the value of the determination coefficient ($R^2 = 0.9335$) was reasonably close to 1. At the same time, a low value of coefficient of the variation (CV = 4.41%) indicated a high degree of precision and reliability of the experimental values.

The P value is used as a tool to check the significance of each coefficient, which in turn may indicate the pattern of the interactions between the variables. The coefficient estimate for the parameter optimization suggested that the independent variables studied (X_2, X_3), all the two quadratic terms (X_1X_1, X_3X_3) and cross product coefficient (X_1X_2) significantly affected the DS of SLBG. The results of ANOVA showed that the reaction time was the most significant single parameter which influence DS followed by reaction temperature and the ratio of CSA/Py.

3.1.2. Optimization of the reaction conditions

The regression model (5) allowed prediction the effects of the three parameters on the DS of SLBG. The relationship between independent and dependent variables was shown in 2D contour and 3D representation of the response surfaces generated by the model. Two variables within experimental range were depicted in 3D surface plots while the other variables kept constant at zero level. Response surfaces provided a visual interpretation of interactions between two tested variables and the relationships between responses and experiment levels of each variable (Liu et al., 2014). The shapes of the contour plots, circular or elliptical, indicate whether the mutual interactions between the variables are significant or not. Circular contour plot indicates that the interactions between the corresponding variables are negligible, while elliptical contour plot indicates that the interactions between the corresponding variables are significant (Muralidhar, Chirumamila, Marchant, & Nigam, 2001).

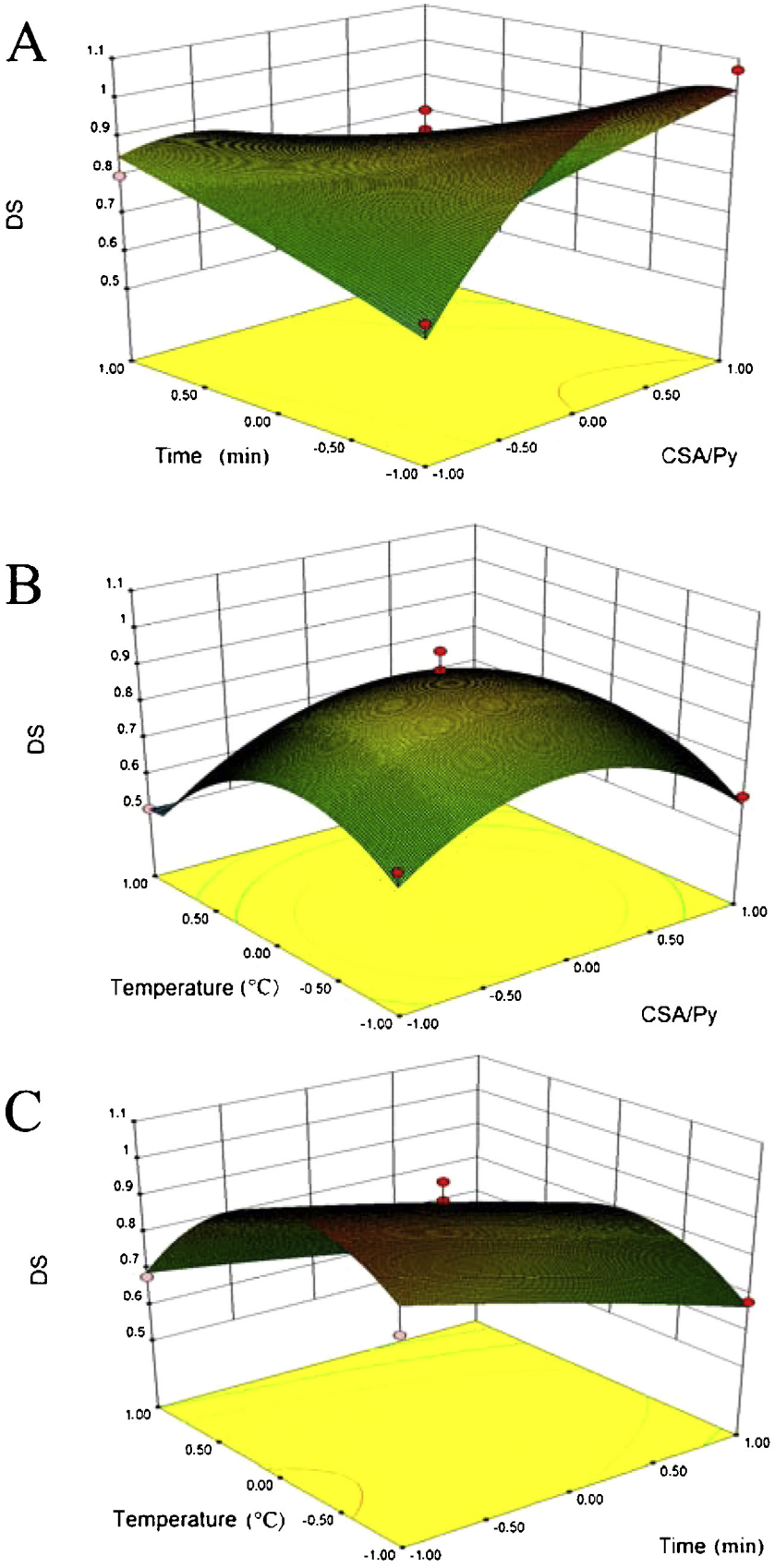

Fig. 1. Response surface for the effects on the DS of SLBG (A) response surface plot for time and ratio of CSA to pyridine; (B) response surface plot for temperature and ratio of CSA to pyridine; (C) response surface plot for temperature and time.

In the present study, three independent response surface plots were shown in Fig. 1. It was clear that the DS of SLBG was sensitive to alterations of the test variables. As shown in Fig. 1A, where the DS of SLBG was given as a function of ratio of CSA/Py (X_1) and reaction time (X_2). It indicated that a high DS can be achieved when the ratio of CSA/Py was 1.27. It was reported that controlling the reagent amount was better than controlling the reaction temperature to obtain sulfated polysaccharide with high DS (Liu et al., 2009). This was in accordance with the previous studies that higher ratio of CSA/Py is benefit to obtain high DS samples (Wang et al., 2009, 2010a). In addition, reaction time (X_2) had a negative impact on the DS of SLBG (Fig. 1A). There was a decrease in the DS with increase in the reaction time (X_2). The surface plots showed that there was a significant interaction between the two parameters. Meanwhile, increased reaction temperature (X_3) up to a threshold level led to a high DS of SLBG. Beyond this level, DS slightly decreased (Fig. 1B). Thus, it might indicate that a medium level of the ratio of CSA/Py and reaction time was required to achieve high DS of SLBG. Lu, Mo, Guo, and Zhang (2012) reported the optimal conditions for sulfation of polysaccharides from persimmon fruits with response surface methodology. They also found that higher DS were obtained at a medium volume ratio (ratio of Py to CSA). However, higher reaction temperature resulted lower DS of SLBG in the studied experimental range (Fig. 1C). This result was in agreement with reports of other authors that hydrolysis or degradation of polysaccharides resulting from the strong acidity of sulfating agent (Lu et al., 2012; Zou et al., 2008; Yang, Du, Huang, Wan, & Wen, 2005a) which was supported by SEC-LLS analysis in Section 3.5.

According to Fig. 1, the optimal reaction conditions of SLBG were as follows: ratio of CSA/Py 1.27, reaction time 120 min and reaction temperature 50.8 °C. Among the three reaction parameters studied, reaction time was the most significant factor to affect DS according to gradient of slope in the 3D response surface plots.

3.1.3. Validation of the models

In order to validate the adequacy of the model equations (Eq. (5)), a verification experiment was carried out under the optimal conditions. Good agreement must exist between the values predicted using the model equations and the experimental values at the points of interest. To ensure the predicted result was not biased toward the practical value, experimental rechecking was performed using this deduced optimal condition (Samavati, 2013; Liu et al., 2014). A mean value of 1.05 ± 0.064 ($n = 5$), obtained from real experiments, demonstrated the validation of the RSM model. The validation result revealed that there was no significant difference between experimental and predicted values, suggesting that the response model was adequate for reflecting the expected optimization. This result of analysis indicated that the experimental values were in good agreement with the predicted ones, and also suggested that the model of Eq. (5) is satisfactory and accurate.

3.2. FT-IR analysis

Fig. 2 shows the FT-IR spectrum of purified LBG, $SLBG_2$, $SLBG_4$ and $SLBG_{14}$ with the DS of 1.07, 0.34 and 0.85, respectively. The bands around 3437 cm^{-1} and 2939 cm^{-1} were due to the hydroxyl stretching vibration and C—H stretching vibration, respectively. With the increasing of DS, the intensity of 2939 cm^{-1} was decreased. New bands at 1251 cm^{-1} described an asymmetrical S=O stretching vibration in SLBG. The region around 800–850 cm^{-1} is used to infer the position of the sulfate group in sulfated polysaccharides. The bands at 845, 830 and 810 cm^{-1} are assigned to 3-sulfate, 2-sulfate and 6-sulfate of D-galactose units, respectively (Jeanny et al., 2008). SLBG showed a moderate intensity bands at 810 cm^{-1} indicating a symmetrical C—O—S vibration which was

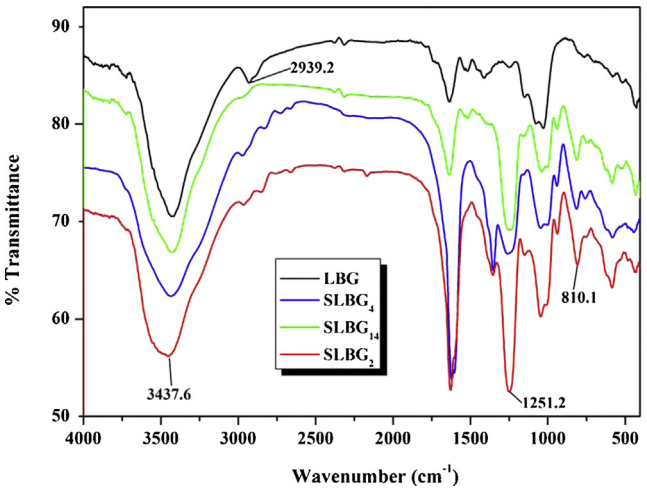

Fig. 2. FT-IR spectra of LBG and its sulfated derivatives in different reaction conditions.

attributed to the sulfate substitution at C-6. It was well known that the reactivity of hydroxyl group was C-6 > C-2 > C-3. The low reactivity of position C-2 and C-3 could be attributed to the steric hindrance (Yang et al., 2005a). The result was also supported by ^{13}C NMR analysis in Section 3.3.

The effect of DS on the FT-IR spectrum of SLBG was also investigated by the peak intensity. As shown in Fig. 2, an increase in DS from 0.37 to 1.07 resulted an increment in the intensity of the bands (1251 cm^{-1} for S=O stretching vibration). In addition, the intensity of the peak at 1043.48 cm^{-1} for C—O—C stretching vibration slightly decreased due to the degradation of the samples during esterification reaction.

3.3. NMR analysis

The ^{13}C NMR spectrum of LBG and $SLBG_2$ was presented in Fig. 3A and B. The anomeric region near 100 ppm showed two main signals, which were assigned as C-1 of α-D-galactose at 95.3 ppm and β-D-mannose at 99.1 ppm. The substitution of α-D-galactose on the (1 → 4)-β-D-mannopyranose main chain was characteristic by the C-4 peaks at 76.4 and 76.2 ppm. Peak at

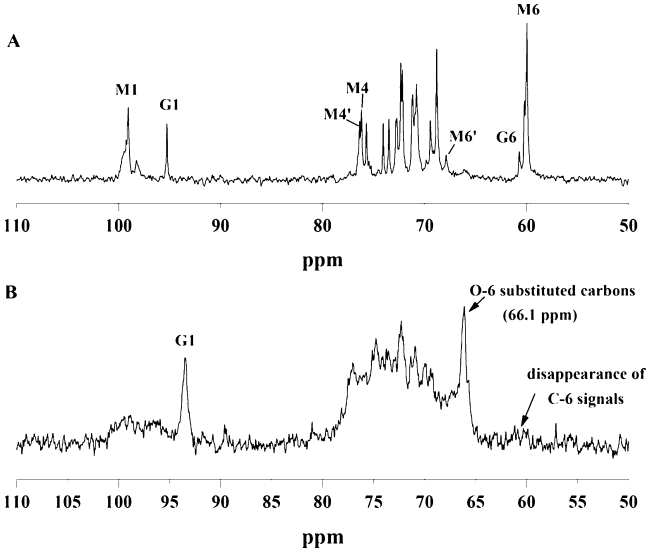

Fig. 3. ^{13}C NMR spectra of LBG (A) and $SLBG_2$ (B). M and G represents mannose and galactose unit, respectively.

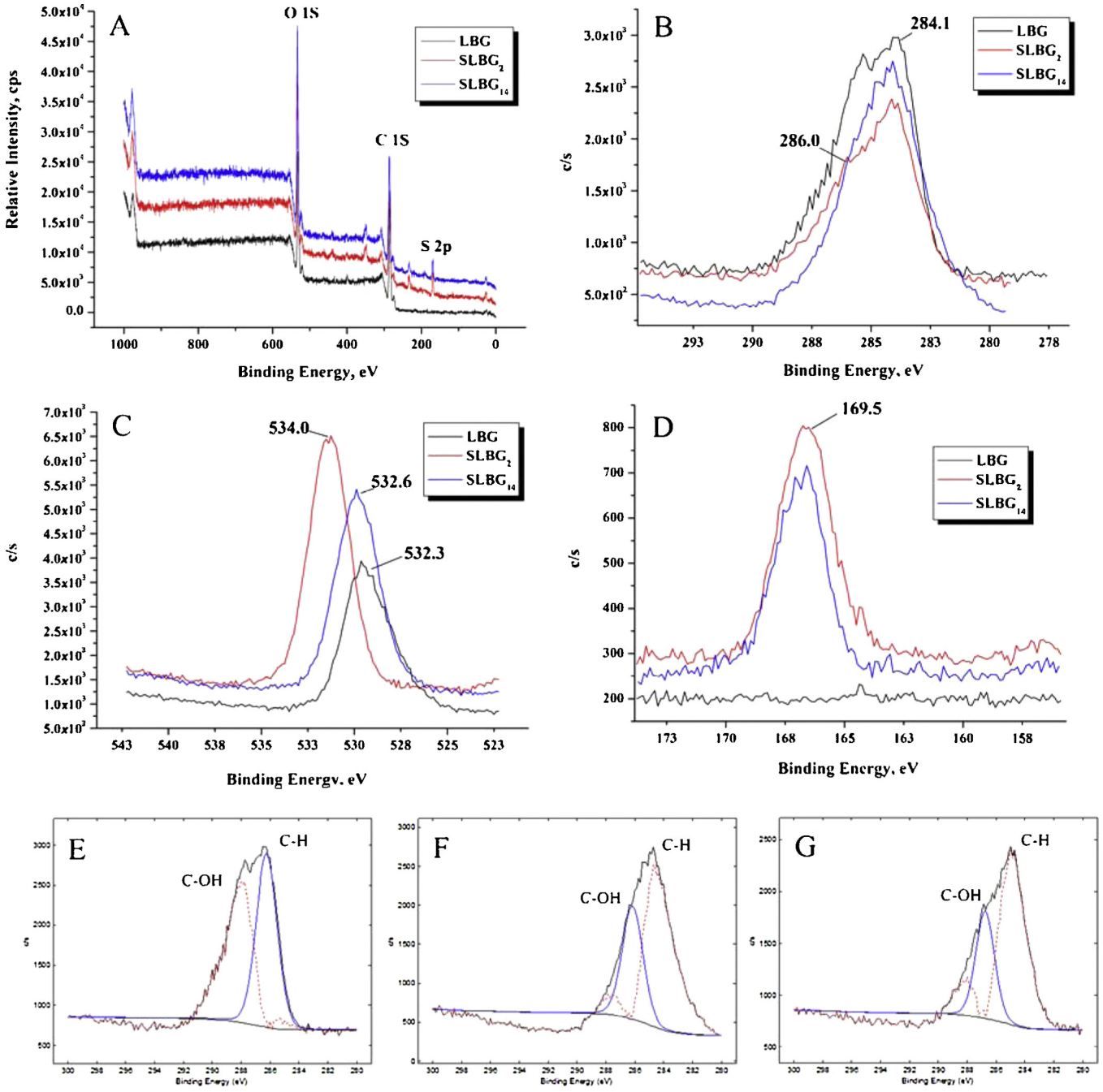

Fig. 4. XPS spectra and curve-fitting of C 1s spectra (A) survey spectra. (B) C 1s spectra. (C) O 1s spectra. (D) S 2p spectra. (E) curve-fitting of LBG (F) curve-fitting of $SLBG_{14}$ and (G) curve-fitting of $SLBG_2$.

76.4 corresponded to two continuous substituted β-D-mannose units while peak at 76.2 was assigned to unsubstituted β-D-mannose units that were adjacent to another residue of the same kind. It was very similar to the results of the ^{13}C NMR spectra reported by Muschin and Yoshida (2012). Our result also showed that resonance from C-4 of D-mannose residues were split, in evident dependence upon the nearest neighbor probabilities of D-galactosyl groups along the mannose chains (Sébastiena et al., 2014). Signals at 59.9 and 60.7 ppm were assigned to C-6 of β-D-mannopyranosyl and α-D-galactose unit. The downfield displacement of the mannose primary group from 59.9 to 67.8 ppm was characteristic of 6-O substitution of α-D-galactose linked to β-D-mannose main chain (Melo, Feitosa, Feitosa, Freitas, & Paula, 2002).

It was found that the ^{13}C NMR spectra became more complicated after sulfation (Fig. 3B) because the carbon directly attached to an electron-withdrawing sulfate group would shift to a lower field position, while the carbon indirectly attached to sulfate group would shift to higher field position (Cunha, Vieira, Arriaga, Paula, & Feitosa, 2009; Yang, Gao, Han, & Tan, 2005b). The new peak at 66.1 ppm of $SLBG_2$ was assigned to the O-6 substituted carbons, suggesting sulfation of O-6 (Melo et al., 2002; Cunha et al., 2009; Cardoso, Noseda, Fujii, Zibettic, & Duartea, 2007). In addition, the disappearance of C-6 signals near 60 ppm indicated that the C-6 OH groups were completely sulfated. It was known that the signal of C-1 splits if OH group on C-2 was functionalized and this splitting of the C-1 signal correlates well with the extent of substitution at the C-2 atom (Yang et al., 2005b). $SLBG_2$ showed a split of the signals at

Table 3
Molecular characterization of LBG and its sulfated derivative by SEC-LLS.

Sample	$M_W \times 10^5$	M_W/M_n	$\langle S^2\rangle_z^{1/2}$ (nm)	Relation equation	d_f	Conformation
LBG	23.13	1.952	91.6	$\langle S^2\rangle_z^{1/2} = -0.982M_w^{0.45\pm0.036}$	2.22	Between hard sphere and random coil (not swollen)
$SLBG_1$	1.250	2.97	27.9	$\langle S^2\rangle_z^{1/2} = 0.360M_w^{0.34\pm0.049}$	2.94	Between hard sphere and random coil (fully swollen)
$SLBG_2$	5.926	2.170	72.6	$\langle S^2\rangle_z^{1/2} = -1.377M_w^{0.54\pm0.019}$	1.85	Random coil
$SLBG_3$	4.229	1.534	57.5	$\langle S^2\rangle_z^{1/2} = -1.523M_w^{0.56\pm0.028}$	1.78	Random coil
$SLBG_4$	0.626	1.898	24.5	$\langle S^2\rangle_z^{1/2} = 0.892M_w^{0.32\pm0.051}$	3.12	Hard sphere
$SLBG_5$	4.811	1.541	79.5	$\langle S^2\rangle_z^{1/2} = -2.326M_w^{0.46\pm0.017}$	2.17	Between hard sphere and random coil (not swollen)
$SLBG_6$	0.893	2.086	42.8	$\langle S^2\rangle_z^{1/2} = -0.077M_w^{0.30\pm0.024}$	3.33	Hard sphere
$SLBG_7$	3.098	1.656	49.8	$\langle S^2\rangle_z^{1/2} = -1.085M_w^{0.43\pm0.022}$	2.32	Between hard sphere and random coil (not swollen)
$SLBG_8$	0.521	1.473	21.6	$\langle S^2\rangle_z^{1/2} = 0.064M_w^{0.28\pm0.051}$	3.59	Hard sphere
$SLBG_9$	3.285	1.834	54.1	$\langle S^2\rangle_z^{1/2} = -1.957M_w^{0.48\pm0.033}$	2.08	Between hard sphere and random coil (not swollen)
$SLBG_{10}$	3.932	1.889	64.9	$\langle S^2\rangle_z^{1/2} = -1.505M_w^{0.56\pm0.029}$	1.78	Random coil
$SLBG_{11}$	0.688	2.021	23.4	$\langle S^2\rangle_z^{1/2} = -0.02M_w^{0.28\pm0.037}$	3.57	Hard sphere
$SLBG_{12}$	0.748	2.031	24.8	$\langle S^2\rangle_z^{1/2} = 0.128M_w^{0.31\pm0.029}$	3.22	Hard sphere
$SLBG_{13}$	1.148	2.295	43.4	$\langle S^2\rangle_z^{1/2} = -1.262M_w^{0.51\pm0.021}$	1.96	Random coil
$SLBG_{14}$	1.534	2.357	44.7	$\langle S^2\rangle_z^{1/2} = -1.881M_w^{0.62\pm0.027}$	1.61	Random coil
$SLBG_{15}$	1.002	2.555	39.2	$\langle S^2\rangle_z^{1/2} = -1.633M_w^{0.48\pm0.029}$	2.08	Between hard sphere and random coil (not swollen)

95–100 ppm for C-1. Obviously, all could be assigned for C-1 either without a sulfate group on C-2 or for C-1 with a sulfate group on C-2.

From the results of ^{13}C NMR spectra, the non-selective sulfation of LBG occurred. The intensity of the signals of the O-substitution carbons and the disappearance of C-6 signals near 60 ppm denoted that C-6 substitution was predominant in SLBG compared with other positions, probably owing to steric hindrance as reported elsewhere (Liu et al., 2009).

3.4. XPS analysis

XPS is a surface-sensitive analysis technique, which is capable of providing both qualitative and quantitative information about the presence of different elements of the samples. Fig. 4 showed the qualitative XPS spectra of purified LBG and its sulfated derivatives. The purified LBG had presented three main elements. The binding energy were 284.1 eV for C, 532.3 eV for O and 400.4 eV for N. Carbon and oxygen originated from the well known carbohydrate composition on polysaccharide samples. The presence of nitrogen originated from protein or glycoprotein complex, which was unavoidable contamination in LBG. Fig. 4A also showed the XPS spectra of LBG after sulfated modification. Apart from C, O and N, additional elements, S (binding energy of 169.5 eV) was observed in SLBG samples when compared with the original LBG. This could be attributed to the addition of CSA/pyridine in LBG solutions. This newly emerged peak resulted from the abundant sulfated group that was widely present in SLBG molecules.

Fig. 4C shows O 1s spectra of both LBG and SLBG. The main component at high binding energy (534.0 eV) was due to sulfate oxygens. Furthermore, a broadening of the O 1s peak upon sulfation was observed in SLBG which in agreement with the work of Essayem, Martin, Riondel, and Vedrine (2007). In the case of the O 1s peak presented a different shape possibly due to a much larger component attributable to oxygen bound to sulfur. The S $2p_{3/2}$ spectra of LBG and SLBG were shown in Fig. 4D. It could be found that data from S 2p3/2 was fitted by a Gaussian function centered at 169.5 eV, which in agreement with the binding energies of S $2p_{3/2}$ in $-SO_3^-$. The high binding energy of the S $2p_{3/2}$ revealed that S was only presented as S^{6+} (Cui, Ma, Wang, & Chen, 2007). Hence, it could be concluded that $-SO_3^-$ existed in SLBG. It was also consistent with the results of FT-IR analysis. However, no S $2p_{3/2}$ signal was detected in LBG.

Fig. 4E-4G also shows the detailed C 1s spectra of LBG before and after sulfated modification. The C 1s spectrum of LBG was shown in Fig. 4E. It was composed of two components centered at binding energies of 284.1 and 286.0 eV, which correspond to C—H and C—O, respectively (Wang et al., 2006). As shown in Fig. 4F and G, lower intensity signal at 286.0 eV corresponded to the reduction of the hydroxyl groups after the sulfated modification of LBG. The elemental surface compositions of the samples were also determined by XPS. The C/O ratio acquired therefore reflected the chemical composition of the polysaccharides. For $SLBG_2$ and $SLBG_{14}$, the C/O ratio was determined as 1.72 and 2.20, which was different from the value of 2.41 for LBG. The decrease in C/O ratio suggested an increase in oxygen content after modification.

3.5. Analysis of molecular properties

The characterization of natural polysaccharides and its derivatives having various chemical components, molar mass and chain conformation was important because of their critical effect on end-use structure–property relations (Cui et al., 2008). The molecular weight and chain conformation of LBG and SLBG were determined by SEC-LLS. The weight average molar mass, M_W, polydispersity (PD, M_W/M_n) and Z-average radius of gyration ($\langle S^2\rangle_z^{1/2}$) were shown in Table 3 for all samples. The SEC-LLS chromatograms patterns of LBG and $SLBG_2$ (with the highest DS of 1.07) were shown in Fig. 5. The radius of gyration, M_W, and PD for LBG were measured to be 91.6 nm, 23.13×10^5, and 1.952, respectively.

Our results showed that SLBG with different DS and molecular weight were obtained by changing the reaction conditions. Compared to the native one, all the samples showed a sharp decrease in M_w due to the extensive degradation of the polysaccharides during the sulfation (Table 3). Relevant structural information and further insight into the nature of the polysaccharide can be obtained by investigating the fractal dimension (d_f) (Tao, Zhang, & Peter, 2006). The d_f value could be determined from the M (M_W) dependence of $\langle S^2\rangle_z^{1/2}$ (radius of gyration) and was defined as the inverse of the exponent ν:

$$\langle S^2\rangle_z^{1/2} \sim M^{\nu} \tag{6}$$

$$d_f = \frac{1}{\nu} \tag{7}$$

On the theory of polymer solutions, the value of d_f was 1 for a rigid rod and linear polymers with Gaussian coil nature had d_f value ranging from 5/3 to 2. A three-dimensional object with a homogeneous density had a mass fractal dimension of 3. The d_f value of monodisperse polymers could be extracted directly from

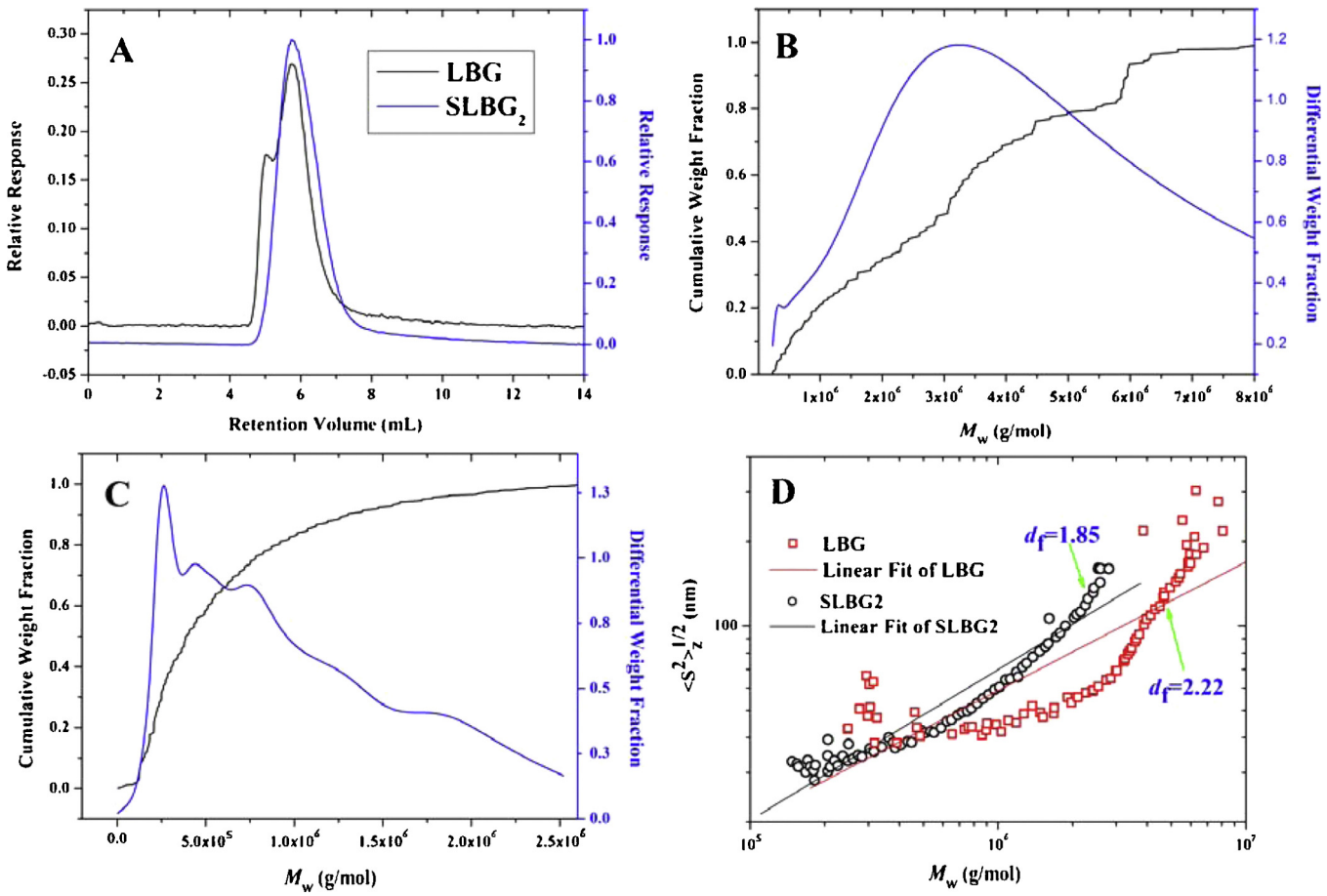

Fig. 5. SEC-LLS chromatograms of LBG and $SLBG_2$ (A) detected by laser light scattering photometry. Molar mass distribution analysis of LBG (B) and $SLBG_2$ (C). Plot of log $\langle S^2\rangle_z^{1/2}$ versus log M_W for LBG and $SLBG_2$ (D). The testing temperature was 25 °C.

the angular dependence of the scattered light or neutron intensity. This approach had been successfully applied to highly branched polysaccharides with high molecular size such as amylopectin and other synthetic branched polymers (Tao & Xu, 2008; Wang et al., 2011).

The straight line fitting of the experimental data points was shown in Table 3. The d_f value of 2.22 suggested that LBG molecules in aqueous solution was characteristic of a particle having an internal structure between the hard sphere ($d_f = 3.0$) and the branched macromolecule in a thermodynamically good solvent (Tao et al., 2006). A fractal dimension of $d_f = 2.5$ was predicted for branched clusters, which were not swollen, either for thermodynamic reasons or because of steric hindrances (Bauer & Burchard, 1993). The result confirmed that LBG existed as a compact chain conformation of branched clusters in aqueous solution.

In sulfated samples, a decrease in d_f values was observed. The d_f values of $SLBG_3$, $SLBG_5$, $SLBG_7$, and $SLBG_{15}$ were 1.78, 2.17, 2.32 and 2.08, respectively. A d_f value of 2.08–2.38 was characteristic of a particle having an internal structure between hard sphere and the branched macromolecules (Bauer & Burchard, 1993). The d_f value of 1.85 indicated that $SLBG_2$ with the highest DS (1.07) exhibited as a random coil conformation in aqueous solution. The result indicated that SLBG with higher DS had a lower ν value. It suggested that DS had greater influence on its conformation in aqueous solution. Our results indicated that sulfated polysaccharides showed less flexibility compared with the native one. It was confirmed by the results of Tao et al. Similar d_f value (1.79) in sulfated polysaccharide showed that the $-SO_3H$ groups in the derivatives enhance the steric hindrance between the polymer chains (Tao et al., 2006).

However, a lower d_f value of 1.61 indicated that $SLBG_{14}$ exhibited as a random coil conformation in aqueous solution. This value was lower than that of $SLBG_2$ with lower DS (0.85) and molecular weight (1.534×10^5). Such a feature could be assigned to the fact that molecular weight were unneglectable in sulfated polysaccharides (Zou et al., 2008). The major driving force for the conformation in aqueous solution was due to the intramolecular hydrogen bonding (Zhang, Li, Wang, Zhang, & Peter, 2011). Low molecular weight and electrostatic effect of $-SO_3H$ groups leading to the relatively expanded conformation of the sulfated derivatives with totally different intramolecular hydrogen bonding compared to the native one. Similar result was reported that the introduction of $-SO_3H$ groups strengthens the effect of electrostatic repulsion, resulting in chain expansion and increased stiffness (Zhang, Zhang, Wang, & Cheung, 2003).

Based on the results, it could be concluded that sulfation and degradation occurred simultaneously in the sulfation process (Parvathy et al., 2005). Higher DS and lower molecular weight might lead to an expanded conformation in aqueous solution. Our earlier result also suggested that the extended chain conformation was beneficial to enhance the antioxidant activities of sulfated polysaccharides in vitro (Wang et al., 2014).

4. Conclusion

In the present study, response surface methodology was proved to be useful for the optimization of the reaction conditions of sulfated LBG. A mathematical model with high fitness was constructed. The optimal reaction conditions of SLBG were: ratio of CSA/Py 1.27,

reaction time 120 min and reaction temperature 50.8 °C. According to the results of XPS, FT-IR and ^{13}C NMR, the sulfation reaction had occurred. The intensity of the signals of the O-substitution carbons denoted that C-6 substitution was shown in SLBG. A decrease in M_w was observed in all samples according to SEC-LLS results. Furthermore, the conformation transition after sulfation was observed in the sulfation process. The results revealed that the introduction of $-SO_3H$ groups improved significantly the stiffness of the chains due to the electrostatic effect. In summary, this work would give an insight that SLBG possessed better physicochemical properties, which will extend the biological applications of this natural polysaccharide.

Acknowledgments

Financial support of this research from National Natural Science Foundation of China (21204073) is gratefully acknowledged. Financial supports of this research from Natural Science Foundation of Gansu Province, China (1308RJZA200) and Promotion Plan of Scientific Research Ability for Young Teachers from Northwest Normal University are also gratefully acknowledged. We would also like to thank Prof. Fengyiny Jing (Chang Chun Institute of Applied Chemistry, Chinese Academy of Science) for the measurement of NMR and Prof. Ruibin Guo (The Key Laboratory of Ecological Environment Related Polymer Materials of Ministry of Education, Northwest Normal University) for the use of SEC-LLS.

References

Barak, S., & Mudgil, D. (2014). Locust bean gum: Processing, properties and food applications–A review. *International Journal of Biological Macromolecules*, *66*, 74–80.

Bauer, J., & Burchard, W. (1993). Determination of scaling properties of randomly branched polycyanurates by combined SEC/LALLS/VISC. *Macromolecules*, *26*, 3103–3107.

Cardoso, M. A., Noseda, M. D., Fujii, M. T., Zibettic, R. G. M., & Duartea, M. E. R. (2007). Sulfated xylomannans isolated from red seaweeds *Chondrophycus papillosus* and *C. flagelliferus* (Ceramiales) from Brazil. *Carbohydrate Research*, *342*, 2766–2775.

Chen, X. Y., Xu, X. J., Zhang, L. N., & Kennedy, J. F. (2009). Flexible chain conformation of (1 → 3)-β-D-glucan from Poria cocos sclerotium in NaOH/urea aqueous solution. *Carbohydrate Polymers*, *75*, 586–591.

Chen, X. Y., Xu, X. J., Zhang, L. N., & Zeng, F. B. (2009). Chain conformation and anti-tumor activities of phosphorylated (1 → 3)-β-D-glucan from Poria cocos. *Carbohydrate Polymers*, *78*, 581–587.

Cui, H. X., Liu, Q., Tao, Y. Z., Zhang, H. F., Zhang, L., & Ding, K. (2008). Structure and chain conformation of a (1–6)-α-D-glucan from the root of *Pueraria lobata* (Willd.) Ohwi and the antioxidant activity of its sulfated derivative. *Carbohydrate Polymers*, *74*, 771–778.

Cui, X., Ma, H. Z., Wang, B., & Chen, H. W. (2007). Direct oxidation of *n*-heptane to ester over modified sulfated SnO_2 catalysts under mild conditions. *Journal of Hazardous Materials*, *147*, 800–805.

Cunha, P. L. R., Vieira, I. G. P., Arriaga, A. M. C., Paula, R. C. M., & Feitosa, J. P. A. (2009). Isolation and characterization of galactomannan from *Dimorphandra gardneriana* Tul. seeds as a potential guar gum substitute. *Food Hydrocolloids*, *23*, 880–885.

Essayem, N., Martin, V., Riondel, A., & Vedrine, J. C. (2007). Esterification of acrylic acid with but-1-ene over sulfated Fe- and Mn-promoted zirconia. *Applied Catalysis A: General*, *326*, 74–81.

Jeanny, S. M., Luciano, S. C., Bartolomeu, W. S. S., Darlio, I. A. T., Freitas, A. L. P., Feitosa, J. P. A., et al. (2008). Structural characterization of cold extracted fraction of soluble sulfated polysaccharide from red seaweed *Gracilaria birdiae*. *Carbohydrate Polymers*, *71*, 559–565.

Liu, Y., Gong, G. L., Zhang, J., Jia, S. Y., Li, F., Wang, Y. Y., et al. (2014). Response surface optimization of ultrasound-assisted enzymatic extraction polysaccharides from *Lycium barbarum*. *Carbohydrate Polymers*, *110*, 278–284.

Liu, Y. H., Liu, C. H., Tan, H. N., Zhao, T., Cao, J. C., & Wang, F. S. (2009). Sulfation of a polysaccharide obtained from *Phellinus ribis* and potential biological activities of the sulfated derivatives. *Carbohydrate Polymers*, *77*, 370–375.

Lu, X. Y., Mo, X. Y., Guo, H., & Zhang, Y. L. (2012). Sulfation modification and anticoagulant activity of the polysaccharides obtained from persimmon (*Diospyros kaki* L.) fruits. *International Journal of Biological Macromolecules*, *51*, 1189–1195.

Melo, M. R. S., Feitosa, J. P. A., Feitosa, A. L. P., Freitas, A. L. P., & Paula, R. C. M. (2002). Isolation and Characterization of souble sulfated polysaccharide from the red seaweed *Gracilaria cornea*. *Carbohydrate Polymers*, *49*, 491–498.

Muralidhar, R. V., Chirumamila, R. R., Marchant, R., & Nigam, P. (2001). A response surface approach for the comparison of lipase production by *Candida cylindracea* using two different carbon sources. *Biochemical Engineering Journal*, *9*, 17–23.

Muschin, T., & Yoshida, T. (2012). Structural analysis of galactomannans by NMR spectroscopy. *Carbohydrate Polymers*, *87*, 1893–1898.

Parvathy, K. S., Susheelamma, N. S., Tharanathan, R. N., & Gaonkar, A. K. (2005). A simple non-aqueous method for carboxymethylation of galactomannans. *Carbohydrate Polymers*, *62*, 137–141.

Prajapati, V. D., Jani, G. K., Moradiya, N. G., Randeria, N. P., & Nagar, B. J. (2013). Locust bean gum: A versatile biopolymer. *Carbohydrate Polymers*, *94*, 814–821.

Samavati, V. (2013). Polysaccharide extraction from *Abelmoschus esculentus*: Optimization by response surface methodology. *Carbohydrate Polymers*, *95*, 588–597.

Sébastiena, G., Christopheb, B., Marioa, A., Pascala, L., Michela, P., & Aurore, R. (2014). Impact of purification and fractionation process on the chemical structure and physical properties of locust bean gum. *Carbohydrate Polymers*, *108*, 159–168.

Tao, Y. Z., & Xu, W. L. (2008). Microwave-assisted solubilization and solution properties of hyperbranched polysaccharide. *Carbohydrate Research*, *343*, 3071–3078.

Tao, Y. Z., Zhang, L., & Peter, C. K. (2006). Physicochemical properties and antitumor activities of water-soluble native and sulfated hyperbranched mushroom polysaccharides. *Carbohydrate Research*, *341*, 2261–2269.

Tao, Y. Z., Zhang, L. N., Yan, F., & Wu, X. J. (2007). Chain conformation of water-insoluble hyperbranched polysaccharide from fungus. *Biomacromolecules*, *8*, 2321–2328.

Wang, A. F., Cao, T., Tang, H. Y., Liang, X. M., Black, C., Salley, S. O., et al. (2006). Immobilization of polysaccharides on a fluorinated silicon surface. *Colloids and Surfaces B: Biointerfaces*, *47*, 57–63.

Wang, L., Li, X. X., & Chen, Z. X. (2009). Sulfated modification of the polysaccharides obtained from defatted rice bran and their antitumor activities. *International Journal of Biological Macromolecules*, *44*, 211–214.

Wang, J. G., Ma, Z. C., Zhang, L. N., Fang, Y. P., Jiang, F. T., & Phillips, J. O. (2011). Structure and chain conformation of water-soluble heteropolysaccharides from *Ganoderma lucidum*. *Carbohydrate Polymers*, *86*, 844–851.

Wang, J. L., Guo, H. Y., Zhang, J., Wang, X. F., Zhao, B. T., Yao, J., et al. (2010). Sulfated modification, characterization and structure–antioxidant relationships of *Artemisia sphaerocephala* polysaccharides. *Carbohydrate Polymers*, *81*, 897–905.

Wang, J. L., Niu, S. F., Zhao, B. T., Luo, T., Liu, D., & Zhang, J. (2014). Catalytic synthesis of sulfated polysaccharides II: Comparative studies of solution conformation and antioxidant activities. *Carbohydrate Polymers*, *107*, 221–231.

Wang, J. L., Zhang, J., Zhao, B. T., Wang, X. F., Wu, Y. Q., & Yao, J. (2010). A comparison study on microwave-assisted extraction of *Potentilla anserine* L. polysaccharides with conventional method: Molecule weight and antioxidant activities evaluation. *Carbohydrate Polymers*, *80*, 84–93.

Wang, J. L., Zhao, B. T., Wang, X. F., Yao, J., & Zhang, J. (2012). Structure and antioxidant activities of sulfated guar gum: Homogeneous reaction using DMAP/DCC catalyst. *International Journal of Biological Macromolecules*, *50*, 1201–1206.

Wu, Y., Li, W., Cui, W., Eskin, N. A. M., & Goff, H. D. (2012). A molecular modeling approach to understand conformation–functionality relationships of galactomannans with different mannose/galactose ratios. *Food Hydrocolloids*, *26*, 359–364.

Yang, L. Q., & Zhang, L. M. (2009). Chemical structural and chain conformational characterization of some bioactive polysaccharides isolated from natural sources. *Carbohydrate Polymers*, *76*, 349–361.

Yang, J. H., Du, Y. M., Huang, R. H., Wan, Y. Y., & Wen, Y. (2005). The structure-anticoagulant activity relationships of sulfated lacquer polysaccharide: Effect of carboxyl group and position of sulfation. *International Journal of Biological Macromolecules*, *36*, 9–15.

Yang, X. B., Gao, X. D., Han, F., & Tan, R. X. (2005). Sulfation of a polysaccharide produced by a marine filamentous fungus *Phoma herbarum* YS4108 alters its antioxidant properties in vitro. *Biochimica et Biophysica Acta-General Subjects*, *1725*, 120–127.

Yi, Y., Zhang, M. W., Liao, S. T., Zhang, R. F., Deng, Y. Y., Wei, Z. C., et al. (2012). Effects of alkali dissociation on the molecular conformation and immunomodulatory activity of longan pulp polysaccharide (LPI). *Carbohydrate Polymers*, *87*, 1311–1317.

Yin, G. H., & Dang, Y. L. (2008). Optimization of extraction technology of the *Lycium barbarum* polysaccharides by Box–Behnken statistical design. *Carbohydrate Polymers*, *74*, 603–610.

Zhang, M., Zhang, L. N., Wang, Y. F., & Cheung, P. C. K. (2003). Chain conformation of sulfated derivatives of β-glucan from sclerotia of *Pleurotus tuber-regium*. *Carbohydrate Research*, *338*, 2863–2870.

Zhang, Y. Y., Li, S., Wang, X. H., Zhang, L. N., & Peter, C. K. C. (2011). Advances in lentinan: Isolation, structure, chain conformation and bioactivities. *Food Hydrocolloids*, *251*, 96–206.

Zou, C., Du, Y. M., Li, Y., Yang, J. H., Feng, T., Zhang, L., et al. (2008). Preparation of lacquer polysaccharide sulfates and their antioxidant activity in vitro. *Carbohydrate Polymers*, *73*, 322–331.